Vacuum 188 (2021) 110158

Contents lists available at ScienceDirect

Vacuum

journal homepage: http://www.elsevier.com/locate/vacuum

The effective reduction of graphene oxide films using RF oxygen plasma treatment

F.M. El-Hossary [a], Ahmed Ghitas [b], A.M.Abd El-Rahman [c,a], M. Abdelhamid Shahat [b,*], Mohammed H. Fawey [a]

[a] Physics Department, Faculty of Science, Sohag University, 82524, Sohag, Egypt
[b] PV Unit, Solar and Space Research Department, National Research Institute of Astronomy and Geophysics (NRIAG), Helwan, Cairo, Egypt
[c] King AbdulAziz University, Jeddah, Saudi Arabia

ARTICLE INFO

Keywords:
Graphene oxide (GO)
Reduced graphene oxide (rGO)
Radio frequency (RF) plasma
XPS
Raman spectroscopy
TGA
Electrical conductivity

ABSTRACT

Graphene Oxide (GO) has attracted strong research interest due to its unique mechanical, thermal, electrical, and magnetic properties. Herein, a simple oxygen plasma process is used as an eco-friendly, novel and effective surface treatment technique to enhance the microstructure, adhesion force, and electrical properties of the GO films. GO films were treated in a plasma oxygen environment at a constant RF power of 300 W and different processing times ranging from 0 to 7 min. X-ray photoelectron spectroscopy (XPS) and Raman spectroscopy are utilized to examine changes in the type of surface groups and the distribution of bonds energy before and after plasma treatment. Additionally, the effect of RF oxygen plasma treatment on other properties, such as thermal stability, surface roughness, contact angle, work of adhesion, wettability, electrical conductivity, and sheet resistance has been studied. XPS data revealed that RF oxygen plasma treatment reduced the amount of oxygen-containing groups (such as epoxides (O–C═O), carbonyls (C–O–C), and carboxyl's (O–C═O) from 48.8% for the as-prepared GO film to 33.56% after 5 min of treatment. In addition, the average surface roughness (Ra) increased from ~7.8 of as-prepared GO film to ~8.7 μm, while the work of adhesion improved to reach 134.84 mN/m. However, with increasing plasma processing time up to 7 min, the thermogravimetric analysis (TGA) of the treated GO film showed a weight loss difference of 51.66%. Furthermore, introducing a high amount of C═O bonds (carbonyl and SP^2 groups of carbon atoms) after plasma treatment improved the electrical conductivity to a value of 0.156 S/m. The current results indicate that the properties of GO can be tuned by varying the degree of oxidation, which may pave the way for new developments in GO-based applications.

1. Introduction

Graphene is a monolayer of carbon atoms detached from inexpensive pure graphite that is packed into 2-D honeycomb lattices [1]. Graphene oxide (GO) is an oxygenated derivative of graphene. It has abundant functional groups of oxygen and can be exfoliated and dispersed easily in different solvents including water [2,3]. Graphene and its derivatives have enormous expectations for usage in many applications, while its low electrical conductivity is still a challenging problem. Therefore, reducing the GO sheets is considered as one of the effective ways to enhance its electrical properties. The reduced graphene oxide (rGO) has a wider range of applications than GO or even pure graphene, such as an electrode for Li-ion batteries [4], photoconductive switching [5], catalyst [6], supercapacitors [7], sensors [8], biological imaging [9], etc. As known, GO can be chemically or thermally reduced to obtain graphene-like properties. Annealing of GO at high temperatures has used as a thermal reduction technique [10]. Likewise, the chemical reduction can be obtained using strong reducing chemicals, such as hydrazine (N_2H_4) [11] and borohydride ($NaBH_4$) [12]. At the same time, these reducing chemical substances are dangerous and environmental pollutants. It has been found that the rGO sheets produced by chemical or thermal reduction have more defects and poor conductivity, which reduces the carrier mobility restricting its usage in the electronic applications [13]. Alternatively, reduction by radio-frequency (RF) plasma discharge is considered as a more effective, safe, rapid reduction technique as well as an environmentally-friendly method, compared to other chemical and thermal techniques [14]. The RF plasma can be generated using a radio-frequency electric field of 13.56 MHz. In this process, with

* Corresponding author.
E-mail address: m.abdelhamid999@gmail.com (M.A. Shahat).

https://doi.org/10.1016/j.vacuum.2021.110158
Received 9 September 2020; Received in revised form 16 February 2021; Accepted 17 February 2021
Available online 2 March 2021

introducing the sample into the plasma reactor, various physical and chemical reactions have been obtained between the material surface and active plasma species and radiations, which leading to modify the material surface properties. Therefore, RF plasma surface treatment has been used to improve the mechanical, electrical, and optical properties of different materials [15–19].

GO is functionalized and reduced by RF plasma treatment in the presence of a reactive gas like nitrogen, oxygen, hydrogen, and fluorine. Plasma treatment in nitrogen allows for the reduction of GO sheets without obtaining aggressive etching of the GO layers and a low number of surface defects [18]. On the other side, plasma fluorination has found to increase the electrical resistance and to lower the etching intensity of the processed GO sheets. Plasma fluorination is a reversible effect at high temperatures [18]. However, the hydrogen plasma technique has used to remove much oxygen during the reduction process of GO sheets compared to the chemical reduction methods [19]. In hydrogen plasma treatment, atomic hydrogen can be produced and removes oxygen groups from the GO films at a lower temperature compared to the thermal reduction [20]. Further, hydrogen plasma treatment might produce high defective rGO [21] and reduce the work function by shrinking the C–O bonds [22].

On the other hand, RF plasma surface modification of carbon materials using oxygen is a commonly used approach and provides surface oxygen functionalities through different interactions between oxygen plasma species and carbon atoms [1]. Further, external carbon atoms can be removed by etching reactions; forming new oxygen based chemical groups onto the modified GO surface. In either case, the carbon surface is only modified [23–25] Moreover, the degree of disorder of graphene lattice defects can be changed by oxygen plasma treatment leading to high changes in the structural properties and reduction of GO [26]. Promising results have been achieved after using oxygen plasma treatment of various carbon-based materials [27–30]. For example, In Ref. [25], oxygen plasma treatment and amine sources have been used for GO modification. The modified GO films exhibited an increase in surface roughness, decreased thickness, and increased transparency (>90%) with low plate resistance values (177–183 Ω/sq) [25]. It has been found that, oxygen plasma surface treatment of GO films increased the oxygen functional groups, electrical conductivity, surface roughness, and the adhesion force on the grey cotton fabrics [27]. After prolonging the treatment time of the oxygen plasma process, chemical functional groups such as quinones and lactones created and led to an increase in the film's electrical conductivity [27]. Furthermore, Zhu et al., 2018 [28] declared that a cold oxygen plasma-treated graphene during the grown process using the CVD technique increased surface roughness and adhesion force, and led to the formation of C–OH and C═O functional groups.

Although oxygen plasma treatment has previously used for surface modification of GO, its effect on GO properties is still poorly understood and large studies are needed to enhance the electrical properties of GO to meet the requirements of new applications. Herein, the RF oxygen plasma surface treatment has been employed to study the effect of processing time on the reduction level of GO films and in turn on their electrical performance. Plasma processing time has been controlled in the range of 0–7 min at a fixed plasma power of 300 W in order to seek optimization for the treatment process and in turn for obtaining good film properties. This was confirmed based on the results obtained from thickness profiles, XPS, Raman spectroscopy, TGA, contact angle, adhesion force, surface roughness, and electrical measurements of the GO films.

2. Experimental details

2.1. Synthesize of GO nanoparticles (NPs)

GO is prepared by oxidizing graphite flakes using a modified Hummers' method. The materials used in the GO preparation process are summarized in Table 1. Firstly, 3 g of graphite precursor are increasingly dropped to 320 ml of a concentrated solution of H_2SO_4 (98% concentration) into a flask placed in a magnetic stirrer. While the stirring is running, 80 ml of H_3PO_4 solution is dropwise gradually into the flask, and the resulted solution is stirred for 2 h. To avoid the reduction process throughout the preparation due to the rapid rise in temperature of the mixture, 18 g of $KMnO_4$ powder, as an oxidizing agent, are poured in batches into the mixture. The reaction of the mixture continued under stirring for 72 h allowing the oxidation of graphite. As a result of the graphite oxidation, the solution color is changed from black to dark green. To terminate the oxidation process and remove the $KMnO_4$, the H_2O_2 solution is added at room temperature (RT) until no further bubbling is observed. The bright yellow color of the resulting suspension indicates a high oxidation level in graphite oxide [30,31]. Finally, the formed GO is washed three times with 1 Molar of HCl aqueous solution [32]. In order to completely remove the remaining acid, it is repeatedly cleaned with distilled water until a pH range of 6–7 is achieved. The brownish-yellow GO powder is obtained after drying the suspension at 50 °C for 3 h.

2.2. Synthesis of GO films

To clean the glass substrate, a dilute acidic solution of HCl is used for chemical etching. Then, it is followed by an extensive water rinse to remove the residual acid. After that, it is sonicated in acetone to remove the organic impurities, and hence, it rinsed with the deionized water. The obtained brownish-yellow GO powder is dissolved in distilled water forming suspension, which is deposited by a spin coating process on glass substrates using the SpinNXG-P1 spin coater machine at 1000 rpm for 30 s. Finally, the obtained films are dried at an elevated temperature of 50 °C for 1 h.

2.3. Plasma surface reduction of GO films

For reduction process, the obtained GO films are exposed to RF oxygen plasma treatment using an inductively coupled plasma (ICP). The schematic diagram of the ICP system is shown in Fig. 1. The film substrate is mounted on a water-cooled copper sample holder of 3.6 cm diameter, which centered in a quartz reactor tube of 50 cm in length and 4.15 cm in diameter. Before the plasma treatment, the tube is evacuated to a base pressure of 2×10^{-3} mbar measured by a Pirani gauge, and then it is supplied by O_2 gas till a working pressure of 0.1×10^{-3} mbar. A copper induction coil of three turns is used to energize the oxygen plasma discharge using a 13.65 MHz RF power generator (model HFS 2500 D) via a tunable matching network. The as-prepared GO films are treated at a different plasma - processing time of 1, 3, 5, and 7 min for a fixed processing power of 300 W. The height between the sample surface and the center of the plasma glow is fairly high enough (7 cm) to ensure the plasma surface treatment for GO films at low temperatures. The treatment temperature is measured during the modification process by a Chromel-Alumel thermocouple, which is attached to the GO film surface. The GO surface temperature is increased from 130 °C to 150 °C by the plasma runtime. It is important to state that the surface modification using oxygen plasma discharge is performed without using any external source of heating. After completing the plasma treatment, the plasma-treated sample is left inside the reactor tube under vacuum for 10 min to cool slowly to the RT before removing it.

3. Characterization techniques

A Thermo Fisher Scientific K-ALPHA X-ray photoelectron spectroscopy (XPS) with a monochromatic Al Kα X-ray source was employed to examine the chemical compositions and surface chemistry of all plasma-treated GO films. XPS data were collected using an excitation source of 1486.6 eV, 400 μm spot size, 50 eV narrow-spectrum, and with 200 eV of pass energy. Herein, the carbon signal detected in the XPS analysis is

Table 1
Materials used in the GO preparation process; all chemical materials were purchased from Sigma Aldrich.

Materials	Sulfuric Acid	Phosphoric Acid	Graphite Precursor	Potassium Permanganate	Hydrogen Peroxide	Hydrochloric Acid	Distilled Water
Chemical formula	H_2SO_4	H_3PO_4	–	$KMnO_4$, 99%	H_2O_2, 30%	HCl, 37%	–

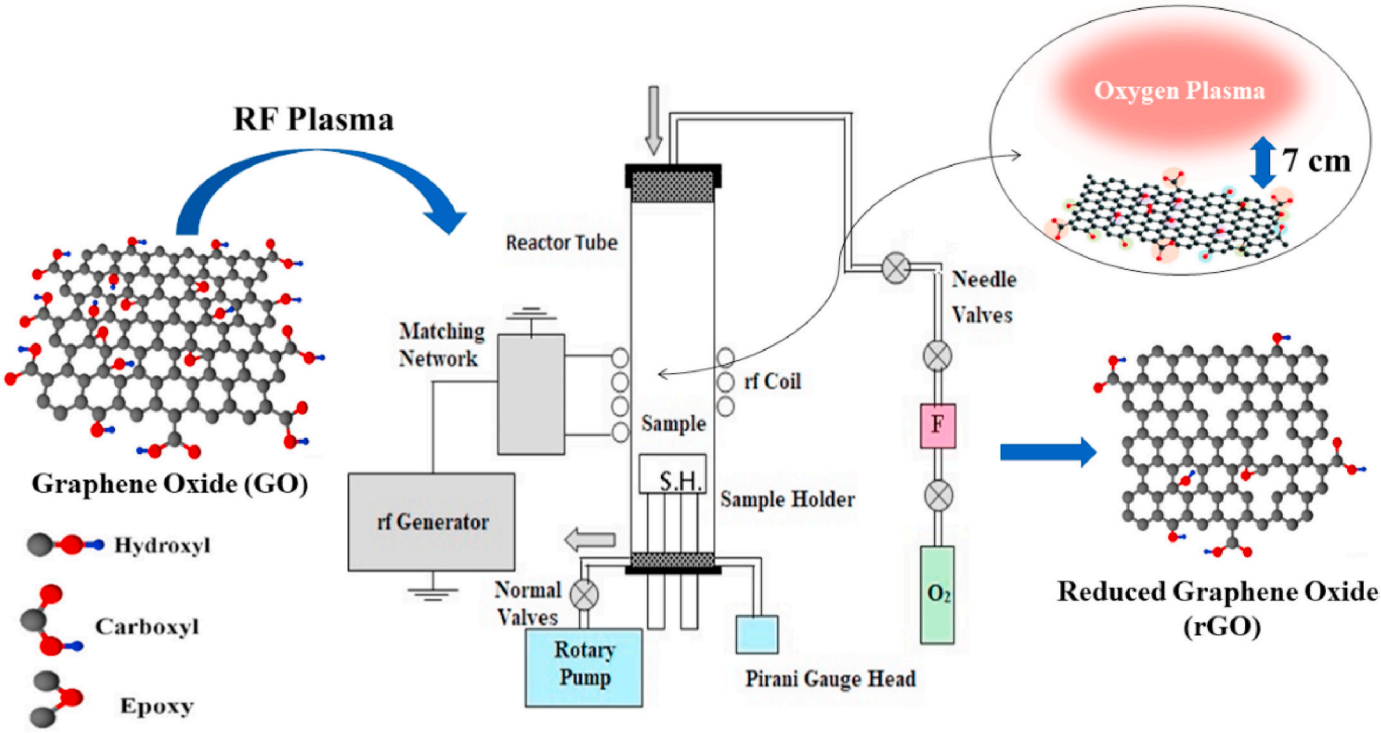

Fig. 1. Schematic diagram of the inductively coupled plasma system (ICP).

mainly referred to the original carbon content in the GO film. Moreover, the signal from possible adventitious carbon on the sample surface is not considered to be a dominant component in the C1s spectrum of GO. As usual, GO is prepared in the lab and mostly composed of sp^2 group, while the sp^3 group was found after chemical oxidation. However, the detection of contaminated carbon can be especially examined as adventitious carbon layers on the metal surfaces before and during the sample preparation or through preserving the samples in an insufficiently evacuated environment [33–35]. To maintain an accurate XPS examination, the spectra were carefully referenced to the C1s line energy of sp^2 type graphitic carbon of GO, which was set at 285 ± 0.1 eV binding energy. A rigorous method for fitting the complex peaks was applied here thus providing more accurate position determinations, i.e. the chemical shift, as well as the integrated intensity of the component peaks representing the various bonding states. A Gaussian-Lorentzian peak form (G/L ratio 70/30) was used for the peak decomposition of O1s and for the reacted C1s lines in this work according to our instrument environment. To get some insight into the chemical composition and structure of the treated GO films, Raman spectroscopy (SENTERRA, Bruker, Germany) with a laser source of 532 nm wavelength has been used. Moreover, a simultaneous DSC/TGA model SDT Q600 (USA) has been employed to study the thermal stability of all treated GO films. The thermogravimetric analysis (TGA) was operated under a nitrogen atmosphere at a temperature range of 25 °C (RT) - 500 °C using a heating rate of 10 °C/min. The surface morphology of all the GO sheets was analyzed using a high-resolution transmission electron microscope (HR-TEM, JEOL JEM-2100) (Japan). A contact angle analyzer (model: SEO Phoenix 300) was used to measure the contact angle, surface tension, wet energy, diffusion of power factor, and the adhesion force. Furthermore, the measurements of surface roughness were carried out using Talysurf 50-Taylor Hopson Precision profilometer. The four-point probe method was applied for measuring the electrical resistance using an EQ-JX2008-LD resistivity tester. For each GO film, the average electrical resistance was calculated from more than 10 readings collected from different points on the film.

4. Results and discussion

4.1. X-ray photoelectron spectroscopy (XPS)

XPS technique has been used to obtain the surface elemental composition of the oxidized GO films, which treated at different processing times of 0, 1, 3, 5, and 7 min. The broad spectra of C1s and O1s acquired from different plasma treated GO samples compared to that of the untreated one are shown in Fig. 2. The XPS spectrum shows different binding energy signals of the untreated and treated samples with higher chemical states at ca.285 eV (graphite C1s) and ca.532 eV (O1s). As observed, the binding energy peak intensity increases gradually with the increase of plasma processing time. Table 2 summarizes the atomic concentration of carbon and oxygen found in the as-prepared and plasma-treated GO films.

As summarized in Table 2, the deconvoluted C1s curve displays six peaks due to C═C and C–C bonding at binding energies in aromatic near C1 (284.8–284.4 eV), SP^2 hybridized carbon atoms near C2 (284.5 eV), C atoms bonded to epoxides (C–O–C) and hydroxyl groups (C–OH) near C3 (286.8–286 eV), carbonyls (C═O) near C4 (287.2 eV), carboxyl groups (O–C═O) near C5 (288.4–288 eV) and π-π* transition loss peak near C6 (292.2 eV) [30–32,36]. On the other side, the O1s spectrum is

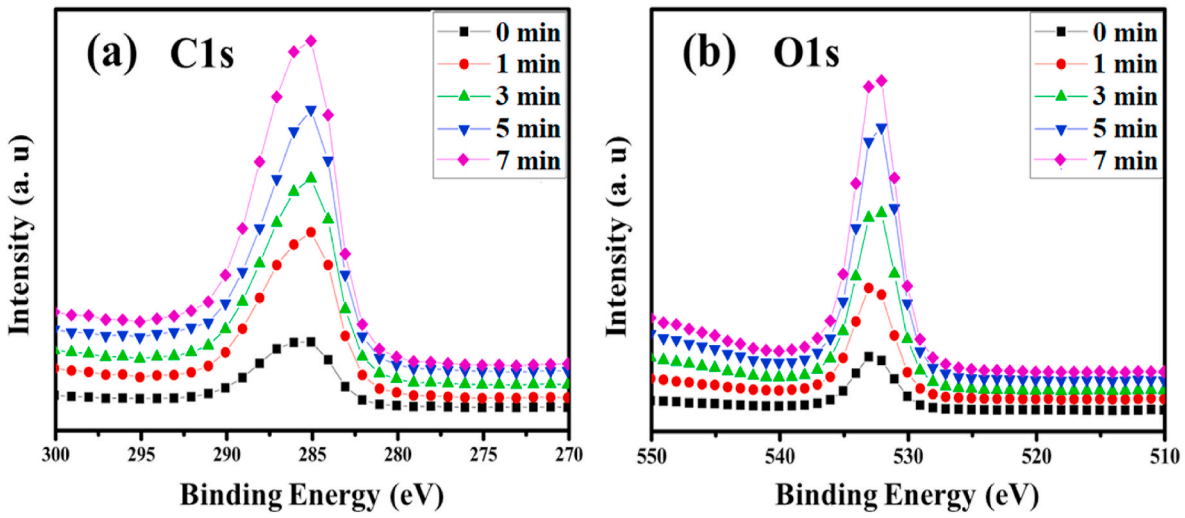

Fig. 2. (a) C1s, (b) O1s XPS spectra of prepared and plasma-treated GO films.

Table 2
Quantity of C1s and O1s (at.%) of the as-prepared and plasma-treated GO films obtained by fitting the XPS spectra.

C1s (%)							O1s (%)	
Binding Energy (eV)	**C1 (284.8–284.4)**	**C2 (284.5)**	**C3 (286.8–286)**	**C4 (287.2)**	**C5 (288.4–288)**	**C6 (292.2)**	**O1 (532.2–531.3)**	O2 (532.7)
Assignment	**Aromatic C–C, C═C**	**Carbon atoms (SP^2)**	**Epoxides (C–O–C)**	**Carbonyls (C═O)**	**Carboxyls (O–C═O)**	***π-π**	**C═O**	C–O
0 min	51.19	–	22.70	26.10	–	–	16.00	84.00
1 min	24.07	33.10	30.70	–	12.12	–	27.41	72.59
3 min	34.00	26.09	17.73	14.31	7.82	–	72.70	27.30
5 min	48.86	–	33.15	–	13.11	4.88	88.66	11.34
7 min	57.37	–	30.45	–	9.27	2.91	100.00	–

divided into two peaks, O1 (532.2–531.3 eV) and O2 (532.7 eV) that are assigned to C═O and C–O, respectively [10,37]. The observed peaks are attributed to the carbon skeleton of GO and the oxygen-containing functional groups in GO films [38,39]. Moreover, the atomic concentrations of carbon and oxygen are calculated from the XPS spectra for as-prepared and plasma-treated GO films (from the ratio of C1s-peak area to the O1s-peak area). Besides, the XPS spectra fitting is very useful to track the evolution of carbon and oxygen groups in prepared and plasma-treated GO films (see Table 2).

As shown in Fig. 3, the quantity of aromatic groups (C–C, C═C) in the C1s spectra decreased from 51.19% for prepared GO to 24.07% after treatment of oxygen plasma for only 1 min, indicating that the carbon - carbon network was disrupted after treatment [27]. It is then increased to the optimum value of 61.65% after treatment for 5 min. Likewise, the quantity of the epoxide groups (C–O–C) gradually increased after exposure to oxygen plasma treatment. New chemical bonds were created after plasma surface treatment such as hybridized carbon atoms (SP^2), carboxyl's (O–C═O), and a small amount of π-π* bonds. The partial disappearance of the small carbonyl group (C═O) indicates the implantation of some amounts of the –OH and –COOH functional groups into GO films after oxygen plasma treatment [29]. The peak of the sp^2 bond is the most distinctive one, demonstrating that most of the carbon atoms reside in honeycomb structures of the graphene lattice [40].

The functional groups C═O and C–O in the deconvoluted O1s spectra shown in Fig. 3 are strongly influenced by the plasma treatment. Gradually increasing the treatment time increases the quantity of C═O from 16% for as-prepared GO to 100% after 7 min of plasma treatment. This can be attributed either to the thermal insulation of the hydroxyl group, which has resulted from the adsorption of water on graphene, or the other oxygen bonds near the edges or defects of the graphene [41].

The corresponding O2 peak to the carbonates and SiO_2 becomes the major component in the films at the higher treating time [36]. Additionally, the as-prepared GO film has a high amount of C–O bond (~84) that gradually decreases by increasing the processing time to disappear at a processing time of 7 min. Increasing the oxygen plasma processing time removes most of the thermally unstable oxygen components in the graphene.

Fig. 4 demonstrates oxygen content ratio in the oxygen-containing groups of (C–O–C), (C═O) and (O–C═O) derived from C1s spectra for the untreated and plasma treated GO films at different processing times of 1, 3, 5, and 7 min. As the plasma processing time increases to 3 min, the amount of oxygen-containing groups (derived from C1s spectra) decreases linearly from 48.8 at.% to 35.17 at.%. Then, it is increased to a maximum value of 46.26 at.% at processing time of 5 min. Afterward, it is decreased to 39.72 at.% at processing time of 7 min. These results demonstrate that the oxygen plasma treatment of GO films has a significant effect on their physical and chemical properties by removing a high amount of oxygen-containing groups from GO surface such as epoxides, carbonyls, and carboxyl's groups [40,41].

4.2. *Raman spectroscopy*

Raman spectroscopy has been used as a powerful and non-destructive spectral technology to characterize the internal structure and surface chemistry changes of as-prepared and treated GO films. Owing to the production of different types of oxygenated function groups at the basal plane and even at the edges, it is likely that the harsh chemical oxidation process causes structural changes in the graphite lattice.

Fig. 5a illustrates the difference in Raman signal spectra of the as-

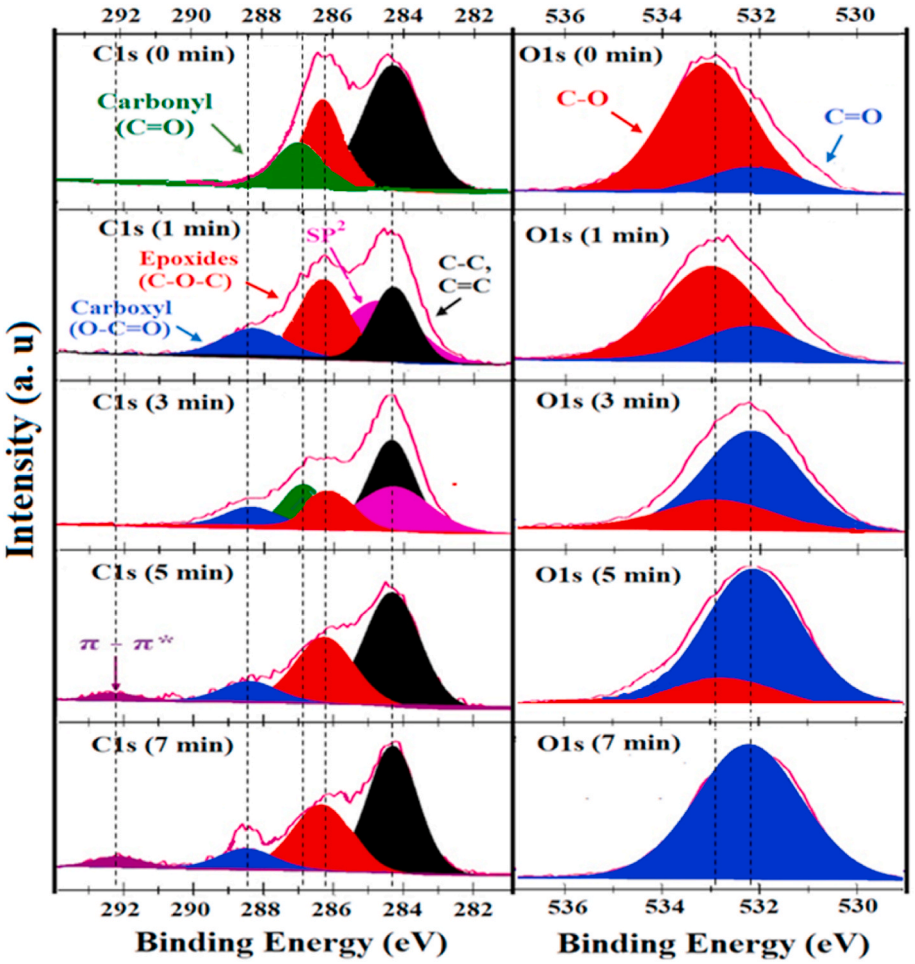

Fig. 3. Deconvoluted C1s and O1s of as-prepared and plasma-treated GO films.

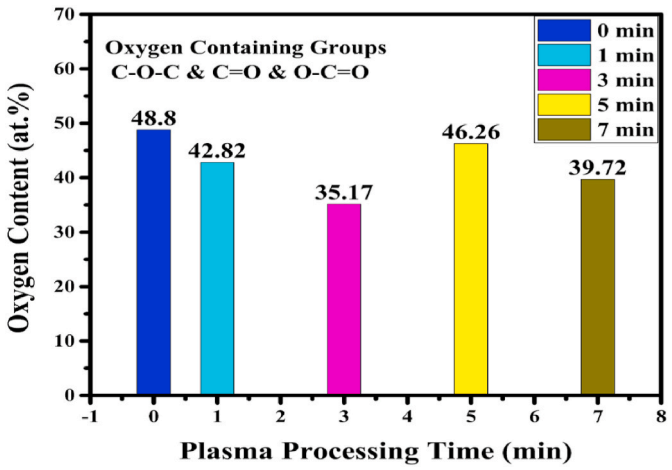

Fig. 4. The ratio of the oxygen content in the oxygen-containing groups of (C–O–C), (C═O) and (O–C═O) derived from the C1s spectra of untreated and plasma treated GO films at different processing times of 1, 3, 5, and 7 min.

prepared and the plasma-treated GO films. The Raman spectra exhibit two prominent peaks located at 1343 cm^{-1} and 1588 cm^{-1} due to the D and G spectral bands, respectively, which show significant changes with respect to the levels of oxidation [42,43]. These peaks are assigned to the dispersive/defect induced vibrations and in-plane vibration mode of sp^2 carbon atoms, respectively. The presence of D-band is due to the first-order scattering of A_{1g}, whereas the G-bands is due to doubly degenerate zone center E_{2g} mode [44].

Due to the oxidation of pristine GO products, the G band is shifted to a higher wavenumber (1601.3 cm^{-1}) after the treatment process. The G-band shift is related to the creation of new sp^2 carbon atoms in the graphite lattice [45]. In addition, the full width half maximum (FWHM) of the G band increases in relation to the oxidation level. As estimated, the FWHM of the G-band was found to be 45, 49, 51, 54 and 52 cm^{-1}, with less defective structures of the treated samples at 0, 1, 3, 5 and 7 min, respectively. The gradual increase in the FWHM values is mostly attributed to the changes in the oxidation levels which indicates an increase in the sp^2 carbons.

Moreover, a higher intensity of Raman signal is obtained from the treated GO film at 3 min for lower surface roughness, and vice versa, the treated GO film at 5 min shows lower intensity of Raman spectra and higher surface roughness. The D band has a comparatively higher intensity which was previously attributed to the creation of defects and disorder such as the presence of in-plane hetero-atoms, grain boundaries, aliphatic chain, etc. [39]. In addition, the nature of the D band can be influenced by the variation of the oxidation levels. As shown, a gradual increase in the oxidation level leads to an increase in the intensity of the D band. The FWHM of the D-band peak is frequently considered to evaluate the surface defect sites. As observed, the FWHM of the D-band peak increases from 86.7 to 100.3 cm^{-1} when the processing time increases from 0 to 5 min, indicating in-plane sp^2 domains in the level of graphene sheets that has a significant influence on the oxidation process with a defective structure [45]. Then, it has decreased to 81.4 cm^{-1} with the plasma processing time increased up to 7 min [3].

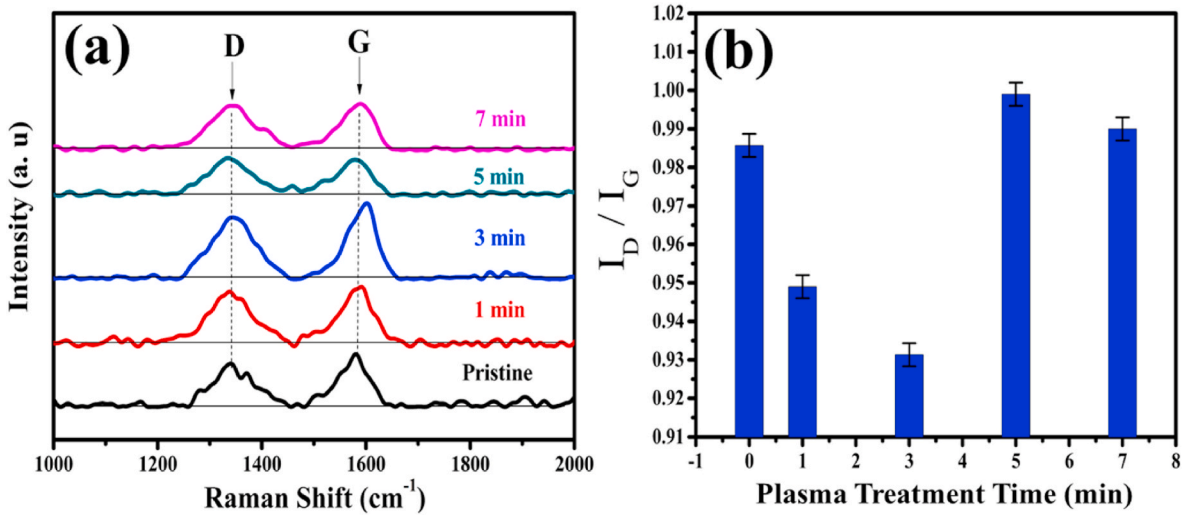

Fig. 5. a) Raman spectra of as-prepared and plasma-treated GO films, b) I_D/I_G ratio versus the processing time.

On the other hand, the relative intensity of the D-band and G-band peaks (I_D/I_G ratio) are affected by the plasma treatment (Fig. 5b). In general, the intensity of the I_D/I_G ratio was systematically decreased for all treated GO films from 0 min to 3 min followed by an increase after 5 min of oxygen plasma treatment (in agreement with the XPS analysis). This increase is attributed to the formation of new defects and disordered or amorphous carbon on the surface of GO owing to the redeposition effect of carbon-based species from the plasma on the surface of the film. Whereas, the decrease in I_D/I_G ratio at higher levels of oxidation is compensated by the increase in the FWHM of the G band. The reduction of functional groups, defect level, and the in-plane sp^2 crystallite size can be estimated from the relative intensity of D and G-band peaks (I_D/I_G) [44,46]. Several studies have been done to improve the defect level I_D/I_G ratio using the plasma treatment of GO films [42,43].

4.3. Thermogravimetric analysis (TGA)

The TGA technique has been employed to study the thermal stability and the functionalization degree of the untreated and treated GO films. Fig. 6 shows the variability of weight loss of untreated and treated GO films in a plasma-nitrogen atmosphere as a function of temperature at different treatment times. As shown, the TGA curves of all investigated samples can be described with three distinguished regions (I, II, and III). Besides, the values of weight loss percent at different temperature ranges are summarized in Table 3. The water molecules absorbed into the GO

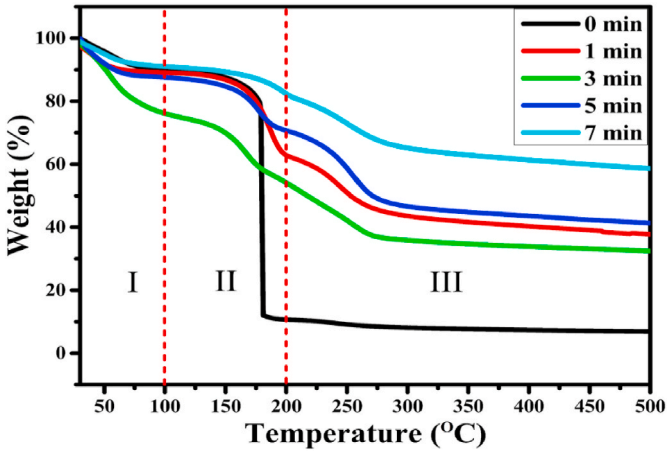

Fig. 6. TGA curves of the as-prepared and plasma-treated GO films.

Table 3
Weight losses of the untreated and plasma-treated GO films calculated from TGA curves.

Temperature (°C)	Weight loss (%)				
	0 min	1 min	3 min	5 min	7 min
30–100	10.12% (0.731 mg)	10.54% (0.192 mg)	24.43% (0.814 mg)	12.86% (0.351 mg)	9.07% (0.414 mg)
100–200	79.2% (5.725 mg)	20.81% (0.379 mg)	18.32% (0.610 mg)	16.22% (0.443 mg)	9.89% (0.451 mg)
200–500	3.82% (0.276 mg)	30.93% (0.5635 mg)	24.86% (0.828 mg)	29.67% (0.812 mg)	22.51% (1.028 mg)
30–500	93.13% (6.732 mg)	62.29% (1.135 mg)	67.62% (2.252 mg)	58.74% (1.604 mg)	41.47% (1.893 mg)

films are evaporated in the first region I (25–100 °C), where they are highly hydrophilic [36]. This causes a material weight loss for the GO films. It was found that the weight loss increased with increasing treatment time and reached a maximum value of 24.43% in 3 min treatment time. This is mainly owing to the creation of additional functional groups (such as carbonyls (C═O) and carbon atoms SP^2) during plasma surface modification. This interpretation is experimentally supported by the XPS analysis. Hence, the weight loss decreases with increasing treatment time and reaches down to a value of 9.07% at a treatment time of 7 min.

Moreover, the pyrolysis of oxygen-containing groups, such as carboxyl and epoxy, can take place in the second region II (100–200 °C) producing CO, CO_2, and H_2O steam [27,47]. In this region, the as-prepared GO film revealed a maximum weight loss of approximately 79.2% at an elevated temperature of 180 °C, indicating a high amount of decomposition of the oxygen-containing functional groups [48]. For the plasma-treated Go films, the weight loss was gradually reduced by increasing the processing time and it reaches to 9.89% at a processing time of 7 min, as summarized in Table 3. This indicates an additional reduction in the functional groups during oxygen plasma treatment. Furthermore, the most stable groups, such as carbonyl and quinone, are decomposed during the third region III (200–500 °C), as well as the pyrolysis of the carbon structure.

Over the temperature range 25–500 °C, the as-prepared GO film revealed a significant weight loss of approximately 93.13%, while the weight loss was reduced in the plasma-treated films to a value of 41.47%

by increasing the processing time to 7 min. The large difference in the features of the TGA curves, as well as in the weight loss of the material before and after plasma treatment, indicates a significant change in the amount of oxygen-containing groups in the GO films during the treatment process, while the thermal stability is preserved for the treated materials. According to the results obtained from the TGA and Raman measurements, the GO film was successfully functionalized and the degree of volumetric reduction for the GO structure was increased by increasing the plasma processing time.

4.4. Morphological characterization

A high-resolution electron transmission microscope (HR-TEM) was used to examine the surface morphology nature of GO treated with different oxidation degree as shown in Fig. 7. As observed from Fig. 7a, the stacked multilayers of the as prepared GO film led to describe the surface as a semitransparent sheet like morphology with minor surface defects. Fig. 7b–c displays a sheet like leaf morphology of a multilayer structure consisting of partially oxidized GO films at low processing times 1–3 min. As illustrated, the GO sheet is observed with a reduced layer number. Further, the film transparency is gradually improved as the plasma treatment time increased. The increased transparency is ascribed to the introduction of functional groups bearing sp^2 hybridized carbon atoms during the oxidation process. A similar effect has been previously detected after oxygen plasma treatment for the GO sheets. The processing effect can be mostly concentrated on removing the unstable oxygen atoms and some amount of functional oxygenated groups from the interplanar of GO sheets such as epoxides, carbonyls, and carboxyl's groups [40,41,49].

As shown in Fig. 7 d-e while the process is increased to relatively longer plasma times (≥5 min), the treatment temperature is increased and led to chemical decomposition of the functional groups which they evaporated to CO and CO_2, i.e., this means that the GO is partially combusted [47]. In details, the treated surface has lower dimensions and higher transparency compared to that of the less oxidized samples (1–3 min). As in agreement with Raman results, the formation of highly oxygenated functional groups (*π-π bonds) with new defects and disordered or amorphous carbon in the treated sheets led to high transparent effect. During the plasma process, the disordered and unwrinkled structure was attributed to the increase in the treatment temperature or via the increase in the mount of oxidant plasma species [50]. Finally, it is suitable to conclude that the leaf morphology, dimensions, and transparency are highly dependent on the oxidation level and plasma etching effect.

4.5. Roughness measurements

The surface roughness of the plasma-treated GO films was changed after oxygen plasma treatment at different times, in which factors such as average roughness (Ra) and root mean surface roughness (Rq) were measured as seen in Fig. 8. Surface roughness is affected by bombardment with fast electrons, ions, and neutral species during exposure to plasma [33]. Accordingly, hills and valleys form after treatment, while on the surface of GO, wrinkles increase.

In the tested region, the surface roughness factors (Ra) and (Rq) of the as-prepared GO film were measured to be ~7.8 and 9.6 μm. Then, the overall Ra and Rq values are decreased by increasing the processing

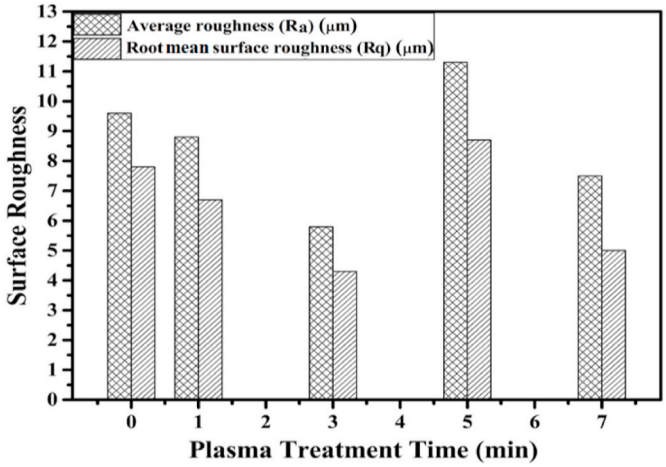

Fig. 8. The surface roughness factors (Ra and Rq) of as-prepared and plasma-treated GO films versus the processing times.

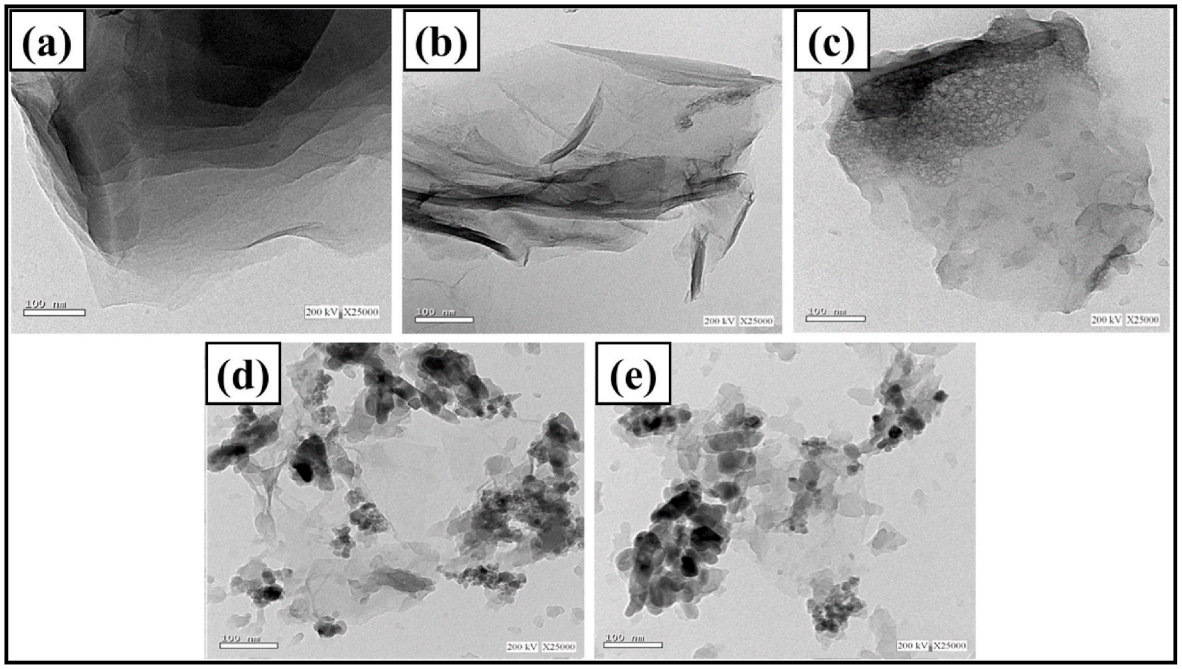

Fig. 7. HR-TEM images of GO with different degrees of oxidation at various processing times. (a) 0 min, (b) 1 min, (c) 3 min, (d) 5 min and (e) 7 min.

time, except for the treated GO film at 5 min (Ra = 8.7 μm and Rq = 11.3 μm). These results are due to changes in the quantities of carbonyl (C–O–C) and epoxides (O–C═O) functional groups on the GO surface, indicating chemical reactions during the treatment process. This indicates the aggregation of surface impurity after treatment, which affects roughness [28]. Moreover, the cooling process forms wrinkles on the surface of the treated GO film due to the surface heat shrinkage. At the same time, the van der Waals forces, which are used to bind the GO film to the substrate, are affected by the heat shrinkage and may form some wrinkle structures [42,51].

4.6. Contact angle

The contact angle (CA), adhesion force, wettability, and water droplet spreading coefficient on the surface of GO films are strongly influenced by oxygen plasma treatment as shown in Fig. 9. The CA of the as-prepared GO film was measured to be approximately 50.45°, indicating that it has hydrophilic properties. After treatment with oxygen plasma, CA of the GO films is gradually increased over treatment time to reach 56.46° at a treatment time of 3 min. Then, the CA value decreased to be 32.28° after 5 min of plasma surface treatment (Fig. 9a). These results can be attributed to the exceptional chemical reactions on the surface of the GO film induced by the high energetic oxygen plasma species, which create vacancies or sites of C–H, SP^3, or OH-bond and in turn produce new defects in the GO films [52]. Meanwhile, the work of adhesion, which represents the adhesion force between the GO films and the droplet water, decreased by increasing the processing time, and hence it increased to 134.84 mN/m after treatment for 5 min (Fig. 9b). The work of adhesion is calculated from the following equation [53]:

$$Wsl = \gamma s + \gamma l + \gamma sl$$

where γs, γ*l*, and γ*sl* are the solid surface free energy, liquid (water) surface free energy, and solid-liquid interfacial energy, respectively. Besides, the Young-Dupré equation is as follows:

$$\gamma s = \gamma sl + \gamma l \cos \theta e$$

Combining the two equations give the next equation [54]:

$$Wsl = \gamma l\,(1 + \cos \theta e)$$

where *θ*e symbolizes to the equilibrium (Young's) contact angle between the oxidized GO films and the droplet of water, while *γl* symbolizes to the water surface tension.

Furthermore, the hydrophilic surface properties of the GO films are affected by the plasma treatment, and hence affecting their wettability and spreading coefficient. The investigation of wettability and spreading coefficient measurements revealed that they are highly dependent on the plasma processing time, as seen in Fig. 9c and d.

4.7. Electrical properties

Today's scientific researchers are interested to improve the electrical properties of GO and rGO. Surface treatment by oxygen plasma has found to be one of the most promising ways to modify the electrical properties of GO and rGO. Therefore, the electrical properties of the GO films before and after oxygen plasma treatment have been investigated. Fig. 10 displays both the electrical conductivity and sheet resistance of the as-prepared GO film and the plasma-treated GO films at different processing times. Sheet resistance was measured by the 4 PP method and

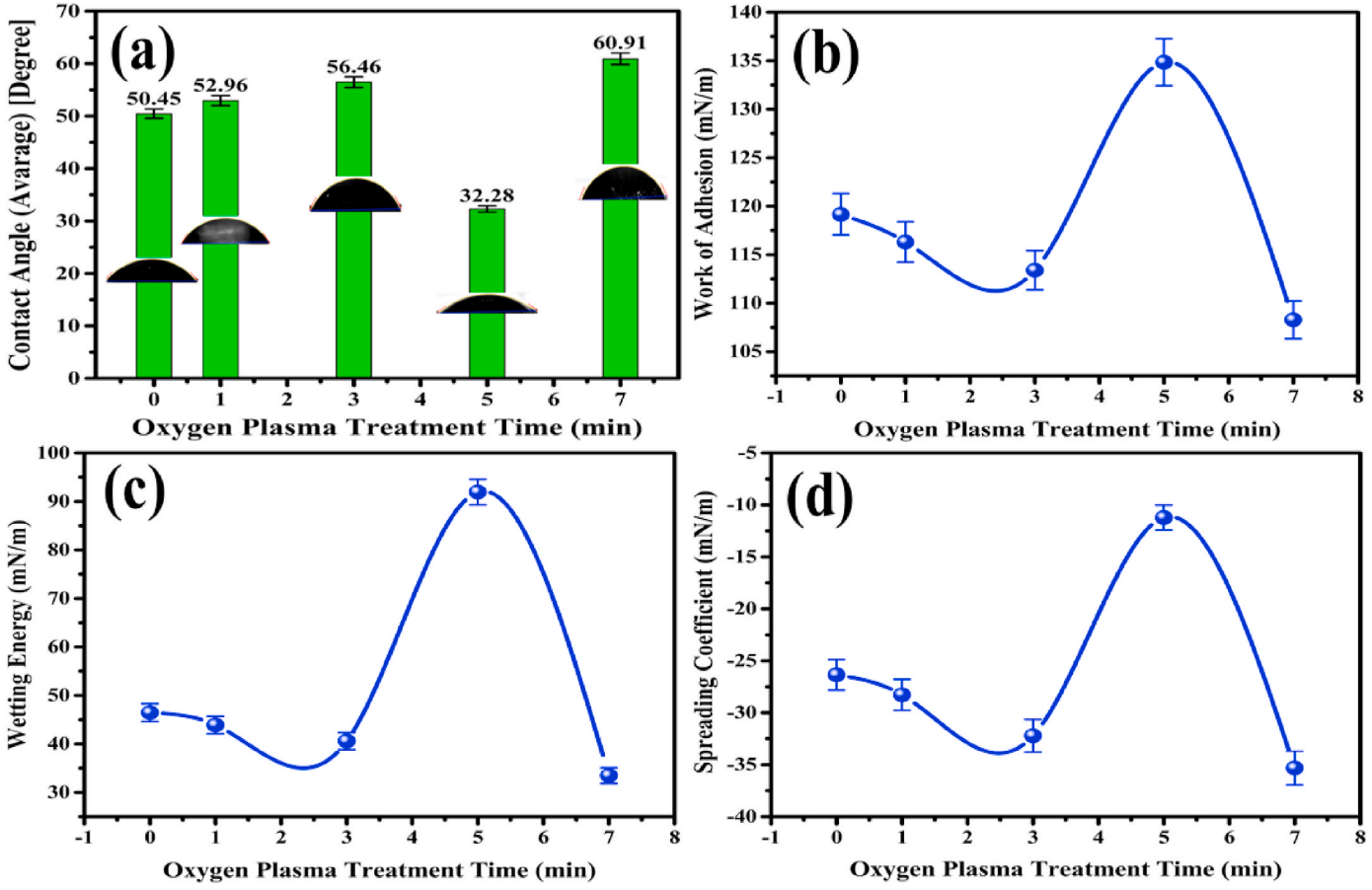

Fig. 9. a) Contact angle, b) Work of adhesion, c) Wetting energy and d) Spreading coefficient curves of as-prepared and plasma-treated GO films at different processing times.

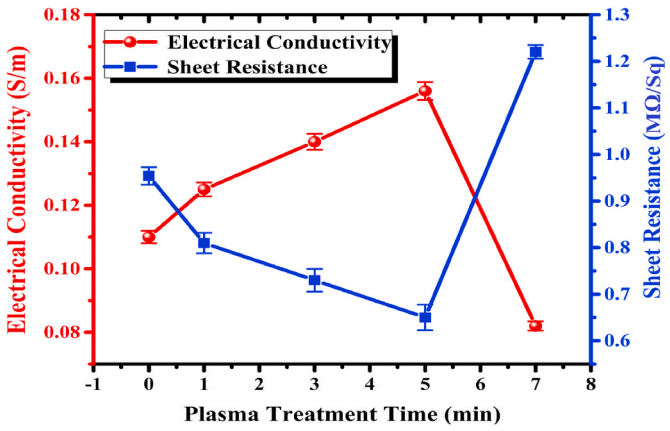

Fig. 10. Electrical conductivity and sheet resistance behavior of the as-prepared GO film and plasma-treated GO films at different processing times.

the values approved that the oxygen plasma treatment has a significant effect on the electrical resistance and conductivity of the GO films. The sheet resistance value of the as-prepared GO film is 0.95 MΩ/square and it gradually decreases over the processing time to 0.65 MΩ/square after 5 min of plasma treatment. The value was then increased over the processing time to reach 1.22 MΩ/square after 7 min of plasma treatment.

Accordingly, the electrical conductivity increased over the processing time from 0.11 S/m for the as-prepared GO film to a maximum value of 0.156 S/m after 5 min of treatment. Then, the electrical conductivity decreased to 0.082 S/m by increasing the processing time to 7 min. According to the XPS and TGA results, the plasma-treated GO films at 1, 3 and 5 min contained a higher amount of (O–C═O) carboxyls and C═O bonds (carbonyl and SP^2 groups of carbon atoms) compared to GO films treated with plasma 7 min. Carbonyl/quinone can facilitate the reactions of oxidation and reduction [46,55,56]. Moreover, the oxygen plasma etching is normally used on the graphene to induce the semiconductor properties. In the current study, the ohmic contact property of graphene does not appear to be destroyed by oxygen plasma etching. The decrease in conductivity by increasing the etching time is owing to the decrease in the number of graphene layers [57] and the lower amount of carbonyl and SP^2 groups of carbon atoms [27,46]. Furthermore, it has been found that the existence of carbonyl/quinone groups in GO can also assist in electron-transporting and enhance the electrocatalytic performance of GO [58]. Whereas the agglomeration of the epoxide and carboxyl functional groups within the GO films and at the same time the presence of oxygenated groups may block the charge carriers and ultimately lead to a deterioration of the electrical conductivity of GO [47,59–61].

5. Conclusion

In summary, oxygen plasma surface treatment has been successfully used to control the reduction degree of GO films. The GO films, synthesized using the modified hummer method, were treated using oxygen plasma at various exposure times (from 0 to 7 min). XPS revealed an increase in the reduction level of the GO films over the processing time from 0 to 5 min by removing a large amount of oxygen-containing groups such as epoxides, carbonyls, and carboxyl's groups. It was found that the amount of oxygen-containing groups decreased from 48.8 at.% to 33.56 at.% after 5 min of plasma processing. The HR-TEM surface morphology for all samples showed a sheet like structure with various transparency. Moreover, the large difference in the features of TGA curves and weight loss between the as-prepared and the treated GO films at 7 min (~51.66%) demonstrated the surface reduction of oxygen-containing groups, while the thermal stability of the materials was preserved. Furthermore, the amount of C═O bonds (carbonyl and SP^2 groups of carbon atoms), which introduced into the GO films after plasma treatment, enhanced the adhesion force between the GO film and the substrate surface. Besides, C═O bonds increased the electrical conductivity of the treated GO films to a maximum value of 0.156 S/m at 5 min of plasma treatment. Finally, oxygen plasma treatment affected the average surface roughness of the treated GO films, where wrinkles were formed on the surface of the treated GO films due to the surface thermal shrinkage.

Declaration of competing interest

We have no conflicts of interest to disclose.

References

[1] Z. Luo, Y. Li, F. Wang, R. Hong, "Plasma exfoliated graphene: preparation via rapid, mild thermal reduction of graphene oxide and application in lithium batteries, Materials 12 (5) (2019) 707, https://doi.org/10.3390/ma12050707.
[2] J.I. Paredes, S. Villar-Rodil, A. Martínez-Alonso, J.M.D. Tascon, "Graphene oxide dispersions in organic solvents, Langmuir 24 (19) (2008) 10560–10564.
[3] D.R. Dreyer, S. Park, C.W. Bielawski, R.S. Ruoff, "The chemistry of graphene oxide, Chem. Soc. Rev. 39 (1) (2010) 228–240.
[4] D. Lin, et al., "Layered reduced graphene oxide with nanoscale interlayer gaps as a stable host for lithium metal anodes, Nat. Nanotechnol. 11 (7) (2016) 626–632.
[5] J. Wei, Z. Zang, Y. Zhang, M. Wang, J. Du, X. Tang, "Enhanced performance of light-controlled conductive switching in hybrid cuprous oxide/reduced graphene oxide (Cu 2 O/rGO) nanocomposites, Opt. Lett. 42 (5) (2017) 911–914.
[6] H. Huang, J. Zhang, L. Jiang, Z. Zang, "Preparation of cubic Cu2O nanoparticles wrapped by reduced graphene oxide for the efficient removal of rhodamine B," J, Alloys Compd. 718 (2017) 112–115.
[7] T. Aytug, et al., "Vacuum-assisted low-temperature synthesis of reduced graphene oxide thin-film electrodes for high-performance transparent and flexible all-solid-state supercapacitors, ACS Appl. Mater. Interfaces 10 (13) (2018) 11008–11017.
[8] E. Singh, M. Meyyappan, H.S. Nalwa, "Flexible graphene-based wearable gas and chemical sensors, ACS Appl. Mater. Interfaces 9 (40) (2017) 34544–34586.
[9] Z. Zang, X. Zeng, M. Wang, W. Hu, C. Liu, X. Tang, "Tunable photoluminescence of water-soluble AgInZnS–graphene oxide (GO) nanocomposites and their application in-vivo bioimaging, Sensor. Actuator. B Chem. 252 (2017) 1179–1186.
[10] C.-M. Chen, Q. Zhang, M.-G. Yang, C.-H. Huang, Y.-G. Yang, M.-Z. Wang, "Structural evolution during annealing of thermally reduced graphene nanosheets for application in supercapacitors, Carbon N. Y 50 (10) (2012) 3572–3584.
[11] I. Jung, et al., "Characterization of thermally reduced graphene oxide by imaging ellipsometry, J. Phys. Chem. C 112 (23) (2008) 8499–8506.
[12] H. Shin, et al., "Efficient reduction of graphite oxide by sodium borohydride and its effect on electrical conductance, Adv. Funct. Mater. 19 (12) (2009) 1987–1992.
[13] W. Yang, C. Wang, "Graphene and the related conductive inks for flexible electronics, J. Mater. Chem. C 4 (30) (2016) 7193–7207, https://doi.org/10.1039/c6tc01625a.
[14] C. Yang, et al., "Fast room-temperature reduction of graphene oxide by methane/argon plasma for flexible electronics, Appl. Surf. Sci. 452 (2018) 481–486.
[15] F.M. El-Hossary, A. Ghitas, A.M. Abd El-Rahman, A.A. Ebnalwaled, M. Abdelhamid Shahat, " characterization and performance of PAni-TiO 2 photovoltaic cells treated by RF plasma, IOP Conf. Ser. Mater. Sci. *Eng.* 956 (2020) 12003, https://doi.org/10.1088/1757-899x/956/1/012003.
[16] F.M. El-Hossary, N.Z. Negm, A.M. Abd El-Rahman, M. Hammad, "Duplex treatment of 304 AISI stainless steel using rf plasma nitriding and carbonitriding, Mater. Sci. Eng. C 29 (4) (May 2009) 1167–1173, https://doi.org/10.1016/j.msec.2008.09.049.
[17] F.M. El-Hossary, N.Z. Negm, A.M.A. El-Rahman, M. Hammad, C. Templier, "Duplex treatment of AISI 304 austenitic stainless steel using rf nitriding and dc reactive magnetron sputtering of titanium, Surf. Coating. Technol. 202 (8) (Jan. 2008) 1392–1400, https://doi.org/10.1016/j.surfcoat.2007.06.066.
[18] E.P. Neustroev, "Plasma treatment of graphene oxide,", Graphene Oxide - Appl. Oppor. (2018) 7, https://doi.org/10.5772/intechopen.77396.
[19] F. Alotaibi, et al., "Scanning atmospheric plasma for ultrafast reduction of graphene oxide and fabrication of highly conductive graphene films and patterns, Carbon N. *Y.* 127 (Feb. 2018) 113–121, https://doi.org/10.1016/j.carbon.2017.10.075.
[20] S.W. Lee, C. Mattevi, M. Chhowalla, R.M. Sankaran, "Plasma-Assisted reduction of graphene oxide at low temperature and atmospheric pressure for flexible conductor applications, J. Phys. Chem. Lett. 3 (6) (Mar. 2012) 772–777, https://doi.org/10.1021/jz300080p.
[21] T. Li, et al., "Plasma treated graphene oxide films: structural and electrical studies, J. Mater. Sci. Mater. Electron. 26 (7) (2015) 4810–4815, https://doi.org/10.1007/s10854-015-3122-0.
[22] P.J. Jesuraj, R. Parameshwari, K. Kanthasamy, J. Koch, H. Pfnür, K. Jeganathan, "Hole injection enhancement in organic light emitting devices using plasma treated graphene oxide, Appl. Surf. *Sci.* 397 (2017) 144–151, https://doi.org/10.1016/j.apsusc.2016.11.110.

[23] I. Junkar, N. Hauptman, K. Rener-Sitar, M. Klanjsek-Gunde, U. Cvelbar, "Surface modification of graphite by oxygen plasma, Inf. MIDEM 38 (4) (2008) 266–271.
[24] U. Rost, et al., "Effect of process parameters for oxygen plasma activation of carbon nanofibers on the characteristics of deposited platinum nanoparticles as electrocatalyst in proton exchange membrane fuel cells," *Int*, J. Electrochem. Sci 11 (2016) 9110–9122.
[25] H. Diker, F. Yesil, C. Varlikli, "Contribution of O2 plasma treatment and amine modified GOs on film properties of conductive PEDOT: PSS: application in indium tin oxide free solution processed blue OLED, Curr. Appl. Phys. 19 (8) (2019) 910–916, https://doi.org/10.1016/j.cap.2019.04.018.
[26] A. Felten, A. Eckmann, J.J. Pireaux, R. Krupke, C. Casiraghi, "Controlled modification of mono-and bilayer graphene in O2, H2 and CF4 plasmas, Nanotechnology 24 (35) (2013) 355705.
[27] I. Kondratowicz, et al., "Tailoring properties of reduced graphene oxide by oxygen plasma treatment, Appl. Surf. Sci. 440 (2018) 651–659.
[28] J. Zhu, H. Deng, W. Xue, Q. Wang, "Effect of low temperature oxygen plasma treatment on microstructure and adhesion force of graphene, Appl. Surf. Sci. 428 (2018) 941–947.
[29] K. Chu, Y. Liu, J. Wang, Z. Geng, Y. Li, "Oxygen plasma treatment for improving graphene distribution and mechanical properties of graphene/copper composites, Mater. Sci. Eng. A 735 (2018) 398–407.
[30] F. M. El-Hossary, A. Ghitas, A. M. Abd El-Rahman, A. A. Ebnalwaled, M. H. Fawey, and M. A. Shahat, "Enhancement of adhesion force and surface conductivity of graphene oxide films using different solvents.".
[31] S. William, J.R. Hummers, R.E. Offeman, "Preparation of graphitic oxide, J. Am. Chem. Soc 80 (6) (1958) 1339.
[32] N.I. Kovtyukhova, et al., "Layer-by-layer assembly of ultrathin composite films from micron-sized graphite oxide sheets and polycations, Chem. Mater. 11 (3) (1999) 771–778.
[33] G. Greczynski, L. Hultman, "C 1s peak of adventitious carbon aligns to the vacuum level: dire consequences for material's bonding assignment by photoelectron spectroscopy, ChemPhysChem 18 (12) (2017) 1507–1512, https://doi.org/10.1002/cphc.201700126.
[34] G. Greczynski, L. Hultman, "Compromising science by ignorant instrument calibration—need to revisit half a century of published XPS data, angew. Chemie - Int. Ed. 59 (13) (2020) 5002–5006, https://doi.org/10.1002/anie.201916000.
[35] G. Greczynski, L. Hultman, "Reliable determination of chemical state in x-ray photoelectron spectroscopy based on sample-work-function referencing to adventitious carbon: resolving the myth of apparent constant binding energy of the C 1s peak, Appl. Surf. Sci 451 (2018) 99–103, https://doi.org/10.1016/j.apsusc.2018.04.226.
[36] S. Tang, et al., "Effective reduction of graphene oxide via a hybrid microwave heating method by using mildly reduced graphene oxide as a susceptor, Appl. Surf. Sci. 473 (2019) 222–229.
[37] C.-H. Huang, T.-H. Lu, "Rapid oxidation of CVD-grown graphene using mild atmospheric pressure O2 plasma jet," *Surf*, Coatings Technol. 350 (2018) 1085–1090.
[38] H.E. Cheng, Y.Y. Wang, P.C. Wu, C.H. Huang, "Preparation of large-area graphene oxide sheets with a high density of carboxyl groups using O2/H2 low-damage plasma, Surf. *Coatings Technol.* 303 (2016) 170–175, https://doi.org/10.1016/j.surfcoat.2016.03.028.
[39] K. Krishnamoorthy, M. Veerapandian, K. Yun, S.-J. Kim, "The chemical and structural analysis of graphene oxide with different degrees of oxidation, Carbon N. Y. 53 (2013) 38–49.
[40] S. Sakulsermsuk, P. Singjai, C. Chaiwong, "Influence of plasma process on the nitrogen configuration in graphene, Diam. Relat. Mater. 70 (2016) 211–218.
[41] I. Bertóti, M. Mohai, K. László, "Surface modification of graphene and graphite by nitrogen plasma: determination of chemical state alterations and assignments by quantitative X-ray photoelectron spectroscopy, Carbon N. Y. 84 (1) (2015) 185–196, https://doi.org/10.1016/j.carbon.2014.11.056.
[42] A.A. Pirzado, et al., "Activation of few layer graphene by μW-assisted oxidation in water via formation of nanoballs–Support for platinum nanoparticles, Colloid Interface Sci. 451 (2015) 221–230.
[43] A.C. Ferrari, "Raman spectroscopy of graphene and graphite: disorder, electron–phonon coupling, doping and nonadiabatic effects, Solid State Commun. 143 (1–2) (2007) 47–57.
[44] M. Aliofkhazraei, N. Ali, W.I. Milne, C.S. Ozkan, S. Mitura, J.L. Gervasoni, Graphene science handbook: electrical and optical properties, First Edition, CRC press, Boka Raton, FL, USA, 2016, pp. 28–35.
[45] A.C. Ferrari, J. Robertson, "Interpretation of Raman spectra of disordered and amorphous carbon, Phys. Rev. B 61 (20) (2000) 14095.
[46] A. Bajpai, R. Sharma, "Atmospheric pressure plasma jet: a complete tool for surface enhanced Raman spectroscopy substrates preparation, Vacuum 172 (2020) 109033.
[47] M. Baraket, S.G. Walton, Z. Wei, E.H. Lock, J.T. Robinson, P. Sheehan, "Reduction of graphene oxide by electron beam generated plasmas produced in methane/argon mixtures, Carbon N. Y 48 (12) (2010) 3382–3390.
[48] D. Romero-Borja, et al., "Organic solar cells based on graphene derivatives and eutectic alloys vacuum-free deposited as top electrodes, Carbon N. Y. 134 (2018) 301–309, https://doi.org/10.1016/j.carbon.2018.03.083.
[49] M. Aziz, F.S.A. Halim, J. Jaafar, "Preparation and characterization of graphene membrane electrode assembly, J. Teknol. (Sciences Eng) 69 (9) (2014) 11–14, https://doi.org/10.11113/jt.v69.3388.
[50] W. Can, Z. Liang, W. Qiao, L. Ling, "Preparation of graphene nanosheets through detonation, New Carbon Mater 26 (1) (2011) 21–25.
[51] Q. Yuan, et al., "Sensitivity enhancement of potassium ion (K+) detection based on graphene field-effect transistors with surface plasma pretreatment, Sensors Actuators B Chem. 285 (2019) 333–340.
[52] J. Robertson, "Diamond-like amorphous carbon, Mater. Sci. Eng. R Reports 37 (4–6) (2002) 129–281.
[53] F. Leroy, F. Müller-Plathe, "Solid-liquid surface free energy of Lennard-Jones liquid on smooth and rough surfaces computed by molecular dynamics using the phantom-wall method, J. Chem. Phys. 133 (4) (2010) 44110.
[54] M. Psarski, D. Pawlak, J. Grobelny, G. Celichowski, "Relationships between surface chemistry, nanotopography, wettability and ice adhesion in epoxy and SU-8 modified with fluoroalkylsilanes from the vapor phase, Appl. Surf. Sci. 479 (2019) 489–498.
[55] S.M. Hafiz, et al., "A practical carbon dioxide gas sensor using room-temperature hydrogen plasma reduced graphene oxide, Sensors Actuators B Chem. 193 (2014) 692–700.
[56] A. Mathkar, et al., "Controlled, stepwise reduction and band gap manipulation of graphene oxide, J. Phys. Chem. Lett 3 (8) (2012) 986–991.
[57] P. Jia, F. Pan, T. Chen, "Effect of oxygen plasma etching on graphene's mechanical and electrical properties, in IOP Conference Series: materials Science and Engineering 182 (1) (2017) 12030.
[58] C. Zhang, S. Chen, P.J.J. Alvarez, W. Chen, "Reduced graphene oxide enhances horseradish peroxidase stability by serving as radical scavenger and redox mediator, Carbon N. Y. 94 (2015) 531–538.
[59] Z. Li, et al., "Raman spectra investigation of the defects of chemical vapor deposited multilayer graphene and modified by oxygen plasma treatment, Superlattices Microstruct 99 (2016) 125–130.
[60] V.B. Mohan, R. Brown, K. Jayaraman, D. Bhattacharyya, "Characterisation of reduced graphene oxide: effects of reduction variables on electrical conductivity, Mater. Sci. Eng. B 193 (2015) 49–60.
[61] N.M. Rodriguez, P.E. Anderson, A. Wootsch, U. Wild, R. Schlögl, Z. Paál, "XPS, EM, and catalytic studies of the accumulation of carbon on Pt black, J. Catal 197 (2) (2001) 365–377.